Journal of Alloys and Compounds 509 (2011) 9312–9317

Contents lists available at ScienceDirect

Journal of Alloys and Compounds

journal homepage: www.elsevier.com/locate/jallcom

Microstructure and electrical properties of $Y(NO_3)_3{\cdot}6H_2O$-doped $ZnO–Bi_2O_3$-based varistor ceramics

Dong Xu[a,b,c,*], Xiaonong Cheng[a], Hongming Yuan[d], Juan Yang[a], Yuanhua Lin[e]

[a] School of Material Science and Engineering, Jiangsu University, Zhenjiang 212013, PR China
[b] Key Laboratory of Semiconductor Materials Science, Institute of Semiconductors, Chinese Academy of Sciences, Beijing 100083, PR China
[c] State Key Laboratory of Electrical Insulation and Power Equipment, Xi'an Jiaotong University, Xi'an 710049, PR China
[d] State Key Laboratory of Inorganic Synthesis and Preparative Chemistry, College of Chemistry, Jilin University, Changchun 130012, PR China
[e] State Key Laboratory of New Ceramic and Fine Processing (Tsinghua University), Beijing 100083, PR China

ARTICLE INFO

Article history:
Received 3 December 2010
Received in revised form 5 July 2011
Accepted 7 July 2011
Available online 22 July 2011

Keywords:
Ceramics
Varistors
Rare earth alloys and compounds
Microstructure
Electrical properties

ABSTRACT

$Y(NO_3)_3{\cdot}6H_2O$-doped $ZnO–Bi_2O_3$-based varistor ceramics were prepared using a solid reaction route. The microstructure, electrical properties, degradation coefficient (D_V), and dielectric characteristics of varistor ceramics were studied in this paper. With increasing amounts of $Y(NO_3)_3{\cdot}6H_2O$ in the starting composition, Y-containing Bi-rich, Y_2O_3, and Sb_2O_4 phases were formed, and the average grain size decreased. Results also showed that with the addition of 0.16 mol% $Y(NO_3)_3{\cdot}6H_2O$, $Y(NO_3)_3{\cdot}6H_2O$ -doped ZnO-based varistor ceramics exhibit comparatively better comprehensive electrical properties, such as a threshold voltage of 425 V/mm, a nonlinear coefficient of 73.9, a leakage current of 1.78 μA, and a degradation coefficient of 1.7. The dielectric characteristics and lightning surge test also received the same additional content of $Y(NO_3)_3{\cdot}6H_2O$. The results confirmed that doping with rare earth nitrates instead of rare earth oxides is very promising route in preparing high-performance $ZnO–Bi_2O_3$-based varistor ceramics.

1. Introduction

Varistors can detect and limit high transient voltage surges and can repeatedly endure such surges [1,2]. They are usually used to sense and limit transient voltage surges. ZnO varistor ceramics show a highly nonlinear current–voltage characteristic with a highly resistive state in the pre-breakdown region that has a large non-linear coefficient [1–10]. Zinc oxide-based varistor ceramics are widely used in electronic appliances, such as voltage surge's protection devices, and especially in high-voltage lines. Commercial varistor ceramics are usually made by a solid state process using ZnO particles with dopant oxides, such as Bi_2O_3, Sb_2O_3, Co_2O_3, MnO_2, and Cr_2O_3. The mixed powder is then pressed and sintered at high temperature. This produces a complex microstructure, in which conducting ZnO grains, an electrically insulating secondary spinel phase, and a Bi-rich inter-granular phase, are attained [11–14].

High-voltage varistor ceramics require a fine-grained microstructure and some methods report the development of high-voltage gradient ZnO varistor ceramics. To reduce ZnO varistor size and increase its voltage gradient, different measures are adopted. In the past, one method decreased the sintering temperature of ZnO varistor ceramics to reduce the growing velocity of ZnO grains, and shortened the temperature-keeping time to decrease the growing time of ZnO grains. However, voltage gradient can only be increased a little. Another method added a suitable amount of Sb_2O_3 to inhibit the growth of ZnO grains. The $Zn_7Sb_2O_{12}$ spinel phase generated in the sintering process is distributed around ZnO grains to inhibit their growth because spinels formed in the grain boundary block the motion of the liquid Bi_2O_3 grain boundary by dragging and pinning effect. Recently, the possibility of improving electrical characteristics by introducing Y_2O_3 to varistor ceramics has been confirmed [15–22]. Bernik et al. [15] investigated microstructural and electrical characteristics of $ZnO–Bi_2O_3$-based varistor ceramics doped with 0–0.9 mol% Y_2O_3. The addition of Y_2O_3 results in the formation of a fine-grained Bi–Zn–Sb–Y–O phase along ZnO grain boundaries, which inhibits ZnO grains growth. The average ZnO grain size decreases from 11.3 to 5.4 mm with an increase in the amount of Y_2O_3. Threshold voltage (V_T) of varistor ceramics increases from 150 to 274 V/mm. The nonlinear coefficient (α) is not influenced and remains at approximately 40. The leakage current (I_L) also increases with the addition of Y_2O_3. Liu et al. [23] reported on $ZnO–Bi_2O_3$-based varistor ceramics doped with 0–3 mol% Y_2O_3. The mean grain size of varistor ceramics decreased from about 9.2 to 4.5 μm, with an

* Corresponding author at: School of Material Science and Engineering, Jiangsu University, Zhenjiang 212013, PR China. Tel.: +86 511 8879 7633.
E-mail address: frank@ujs.edu.cn (D. Xu).

0925-8388/$ – see front matter © 2011 Elsevier B.V. All rights reserved.
doi:10.1016/j.jallcom.2011.07.015

Table 1
Density and electrical properties of $Y(NO_3)_3{\cdot}6H_2O$ doped ZnO–Bi_2O_3-based varistor ceramics.

Sample	D (%)	V_T (V/mm)	d (μm)	V_{gb} (V)	α	I_L (μA)	D_V (%)
YD0	94.5	340	8.00	2.72	27.1	1.60	–
YD1	93.5	339	6.99	2.37	52.8	0.93	3.1
YD2	94.8	425	6. 16	2.62	73.9	1.78	1.7
YD3	94.9	535	4.99	2.67	48.1	2.73	74.0
YD4	93.6	679	3.99	2.71	12.7	25.80	86.1

increase in Y_2O_3 from 0 to 3 mol%. The corresponding varistor's V_T markedly increased from 462 to 2340 V/mm, whereas α decreased from 22.3 to 11.5. However, although some rare earth oxides, such as La_2O_3, Er_2O_3, Lu_2O_3, and Dy_2O_3, were used to improve the electrical characteristics of ZnO–Bi_2O_3-based varistor ceramics, their nonlinearity deteriorated [15,24].

In this paper, the effect of $Y(NO_3)_3{\cdot}6H_2O$ (abbreviated as YN) on the microstructure and the electrical response of ZnO–Bi_2O_3-based varistor ceramics is studied, and the mechanism by which this doping improves the electrical characteristics of ZnO–Bi_2O_3-based varistor ceramics, especially nonlinearity, is discussed.

2. Experimental procedures

Reagent-grade raw materials were used in the proportions (96.5-x) mol% ZnO, 0.7 mol% Bi_2O_3, 1.0 mol% Sb_2O_3, 0.8 mol% Co_2O_3, 0.5 mol% Cr_2O_3, 0.5 mol% MnO_2, and x mol% YN, for x = 0, 0.04, 0.16, 0.40 and 2.00 (samples labeled YD0, YD1, YD2, YD3 and YD4, respectively). After milling, the mixture was dried at 70 °C for 24 h, then the powder was calcined at 700 °C for 2 h in air. The calcined powder mixture was milled again for 1 h to eliminate large powder lumps. The powders were then dried and pressed into discs of ~12 mm diameter and thickness of 2.0 mm. The pressed disks were sintered in air at 1100 °C (2 h dwell time), using a heating rate of 5 °C/min and then cooled in the furnace. The sintered samples were lapped and polished and then the final samples were about 10 mm in diameter and 1.0 mm in thickness. The bulk density of the samples was measured in terms of their weight and volume [25,26].

For the characterization of DC current–voltage, the silver paste was coated on both faces of samples and the silver electrodes were formed by heating at 600 °C for 10 min. The electrodes were 5 mm in diameter. The voltage–current (V–I) characteristics were measured using a V–I source/measure unit (CJP CJ1001). The nominal varistor voltages (V_N) at 0.1 and 1.0 mA were measured and the threshold voltage V_T (V/mm) ($V_T = V_N(1\text{ mA})/t$; t is the thickness of the sample in mm) and the nonlinear coefficient α ($\alpha = 1/\log(V_{1\text{ mA}}/V_{0.1\text{ mA}})$) were determined. The leakage current (I_L) was measured at 0.75 V_N (1 mA) [12,13,16,27–31]. The lightning surge test of YN doped ZnO–Bi_2O_3-based varistor ceramics was measured by short duration shocks of 1 kA, 8/20 μs, and the degradation coefficient D_V, $D_V = 100(|V_{sb} - V_{sa}|)/V_{sb}$, where V_{sb} and V_{sa} are the respective threshold voltages before and after degradation by short duration shocks of 1 kA. The dielectric characteristics [32], such as the apparent dielectric constant (ε) and dissipation factor ($\tan\delta$) were measured as a function of frequency (1 kHz to 10 MHz) and at room temperature using an HP4294A impedance analyzer (Agilent).

The surface microstructure was examined by a scanning electron microscope (SEM, FEI QUANTA 400). The average grain size (d) was determined by the linear intercept method, given by $d = 1.56L/MN$, where L is the random line length on the micrograph, M is the magnification of the micrograph, and N is the number of the grain boundaries intercepted by lines. The crystalline phases were identified by an X-ray diffractometry (XRD, Rigaku D/max 2200, Japan) using a Cu Kα radiation.

3. Results and discussion

Crystalline phases identified by powder XRD and spectra of samples doped with and without various amounts of YN, sintered at 1100 °C for 2 h, are shown in Fig. 1. ZnO–Bi_2O_3-based varistor ceramics typically consist of ZnO grains, spinel, and intergranular Bi-rich phase. In the sample without YN, the ZnO, $Zn_7Sb_2O_{12}$-type spinel, the $Bi_3Zn_2Sb_3O_{14}$, and the Bi_2O_3 phases are identified. However, in the samples doped with YN, the peak of the $Zn_7Sb_2O_{12}$-type spinel phase becomes weaker with the addition of YN [24], nearly vanishing when the amount of YN is increased to 2.00 mol%. With an increase in the amounts of YN in the starting composition, the Y-containing Bi-rich phase ($Bi_{1.9}Y_{0.1}O_3$ phase according to JCPDF 39-0275), the Y_2O_3 phase, and the Sb_2O_4 phase are revealed using XRD analysis. This is so because the addition of YN affects the time that the mixture spends in the liquid phase and, as this becomes longer, the vaporization of Bi_2O_3 from ZnO–Bi_2O_3-based varistor ceramics becomes significant [12,27,33,34]. In the meantime, doping with YN affects the formation and decomposition of $Bi_3Zn_2Sb_3O_{14}$ pyrochlore, which promotes the generation of new phases, such as the Y-containing Bi-rich phase, the Y_2O_3 phase, the Sb_2O_4 phase, and so on.

Figs. 2 and 3 show microstructures of ZnO–Bi_2O_3-based varistor ceramics doped with various amounts of YN. As the concentration of YN increases, average grain size is significantly reduced, from 7.98 to 3.99 μm. At the same time, crystallite sizes of the Y_2O_3 phases become smaller but the quantities increase dramatically, slightly different from the sample without YN doping. Majority of the new phases are much more segregated at multiple ZnO grain junctions than between two ZnO grains. Inasmuch as the diameter of a rare earth cation is larger than that of a Zn^{2+} cation, it is possible that the Yttrium cation was not properly dissolved in the ZnO grains. With an increase in YN content, the Y-rich phase becomes more distributed at multiple ZnO grain junctions, and the Y-rich phase between two ZnO grains is more discontinuously distributed [16,24,35]. At the same time, the size of ZnO grains decreases uniformly when the amount of YN increases, which has some influence on the electrical properties of varistor ceramics. In summary, YN doping can inhibit grain growth, just like rare earth oxides.

The influence of YN concentration on characteristics, including relative density (D), V_T, α, I_L, and degradation coefficient (D_V) of ZnO–Bi_2O_3-based varistor ceramics sintered at 1100 °C for 2 h, is presented in Table 1.

Doping with YN has little influence on the density of ZnO–Bi_2O_3-based varistor ceramics. With an increase in YN concentration, D increases slightly from 93.5% to 94.9%. This trend is similar to D for Y_2O_3-doped ZnO–Bi_2O_3-based varistor ceramics, the difference being that D of Y_2O_3-doped ZnO–Bi_2O_3-based varistor ceramics is higher than D of YN-doped ones [36]. This may be because YN makes the composition more uniform, and the average ZnO grain size becomes very fine. The very fine grain size gives birth to more

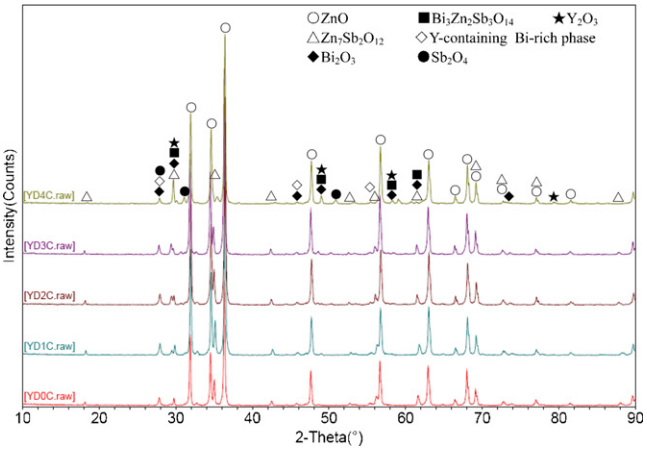

Fig. 1. XRD patterns of ZnO–Bi_2O_3-based varistor ceramics doped with various amounts of $Y(NO_3)_3{\cdot}6H_2O$.

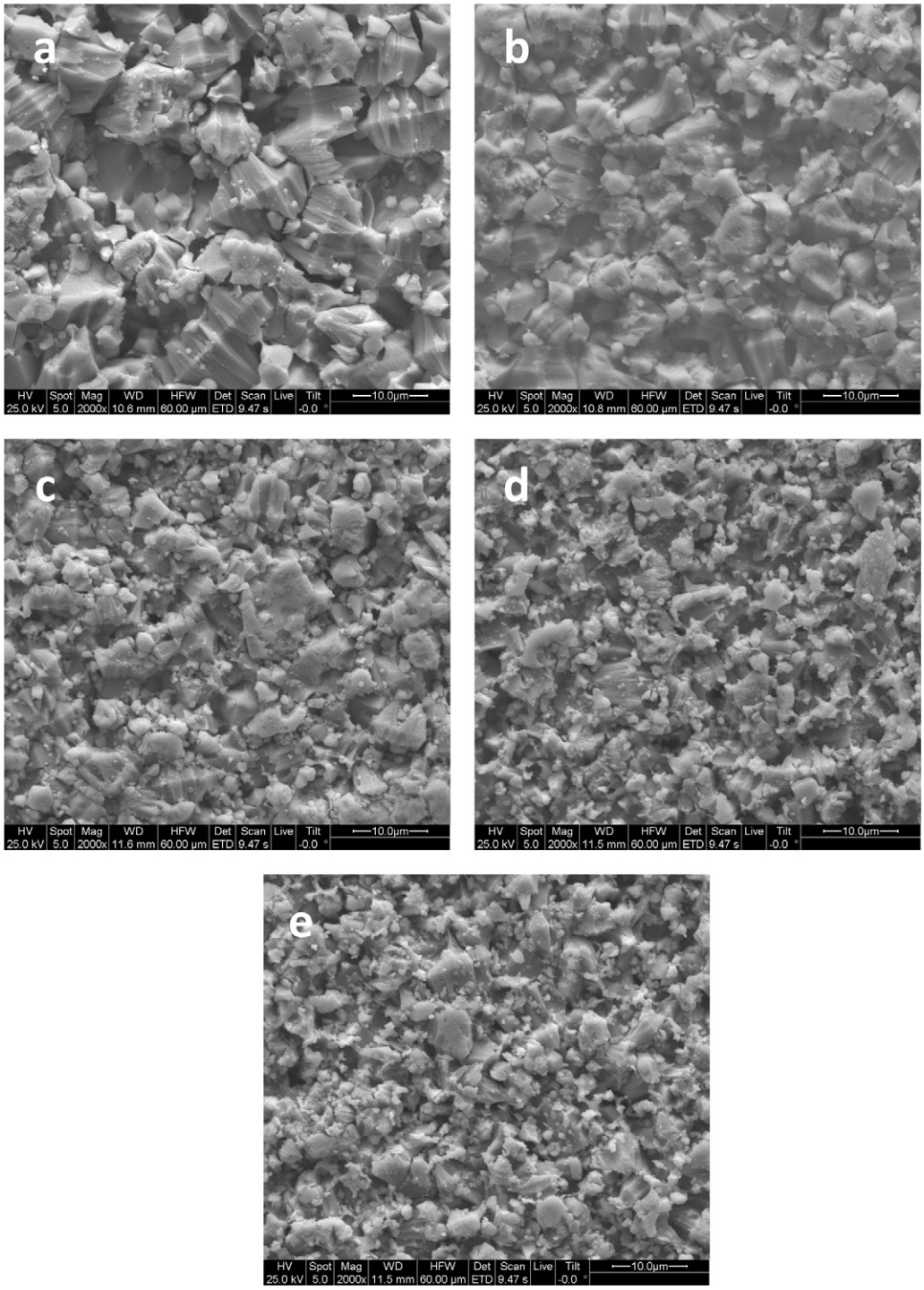

Fig. 2. SEM of ZnO–Bi_2O_3-based varistor ceramics doped with various amounts of $Y(NO_3)_3{\cdot}6H_2O$ (a) YD0; (b)YD1; (c) YD2; (d) YD3 and (e) YD4.

porosity during the sintering of YN-doped ZnO–Bi_2O_3-based varistor ceramics. This may be attributed to the decomposition of YN during sintering. The subsequent porosity of YN-doped varistor ceramics increases.

With an increase YN concentration, V_T is markedly increased in the range of 340–679 V/mm along with a decrease in average grain size of ZnO (Figs. 2 and 3). At the same time, breakdown voltages per grain boundary (V_{gb}) of the samples are all in the range of 2–3 V, according to reports [37,38]. V_{gb} is determined based on the expression $V_{gb} = V_{1\,mA}/n = dV_T$, where n is the number of grain boundaries arranged as the series between both electrodes, and d is the average grain size. However, change in the value of V_{gb} for YN-doped ZnO–Bi_2O_3-based varistor ceramics is different from V_{gb} of Y_2O_3-doped ZnO–Pr_6O_{11}-based varistor ceramics [35]. The difference possibly arises from the microstructure. There are only two phases in Y_2O_3-doped ZnO–Pr_6O_{11}-based varistor ceramics, and more than two phases in YN-doped ZnO–Bi_2O_3-based varistor ceramics. V_{gb} of YN-doped ZnO–Bi_2O_3-based varistor ceramics first decreases then increases, reaching a minimum when doped with 0.04 mol% YN.

The value of α for varistor ceramics without YN is only 27.1, whereas α values of varistor ceramics with YN are in the range of

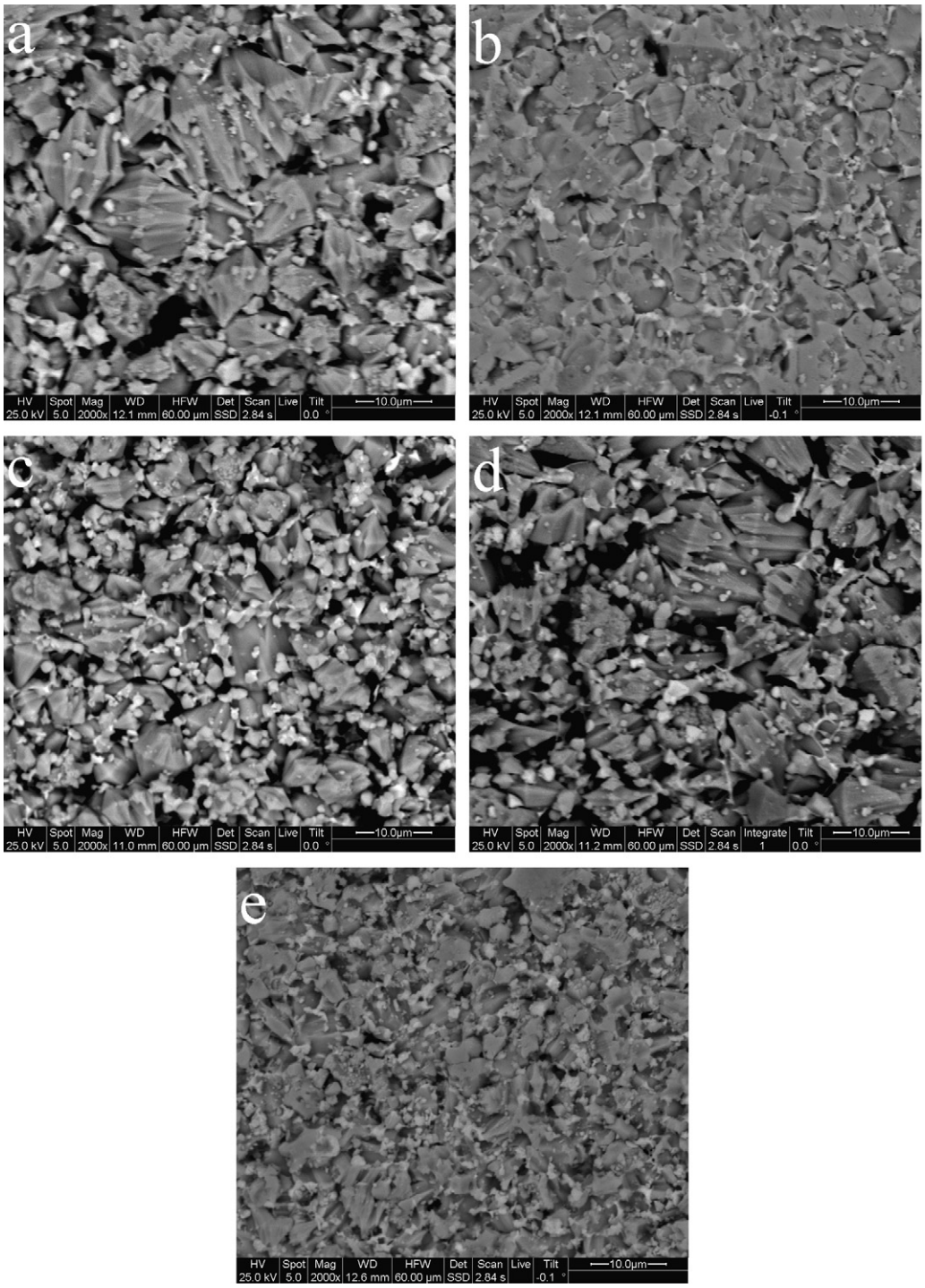

Fig. 3. Backscattered electron (BE) images of ZnO–Bi_2O_3-based varistor ceramics doped with various amounts of $Y(NO_3)_3{\cdot}6H_2O$ (a) YD0; (b)YD1; (c) YD2; (d) YD3 and (e) YD4.

48.1–73.9, achieving a maximum (YD2, 73.9), which is 273% higher with respect to the composition of YD0 (varistor ceramics without YN) with the addition of 0.04–0.40 mol% YN. When YN concentration is higher than 0.40 mol%, α decreases abruptly with an increase in YN doping. The incorporation of YN (0.04–0.40 mol%) can increase α significantly. The significant improvement of α obtained for varistor ceramics with YN is accounted for by microstructure uniformity and narrowed grain size distribution compared with varistor ceramics without YN.

When the amount of YN is more than 0.40 mol%, the number of the spinel phase and the Y-containing Bi-rich phase is increased significantly. The size of the spinel phase and the Y-containing Bi-rich phase becomes smaller and smaller. Then, microstructure uniformity becomes worse and α decreases, which may be related to the formation of the Y-containing Bi-rich phase, which affects the distribution of other dopant cations along the grain boundary. With the formation of the Y-containing Bi-rich phase with traces of other added oxides in YN-doped samples, the concentration and the distribution of Bi_2O_3 and other additives in the grain boundary are modified. Nevertheless, Bi_2O_3 is considered an essential additive that improves nonlinear characteristics. As a result, α deteriorates in the samples doped with YN.

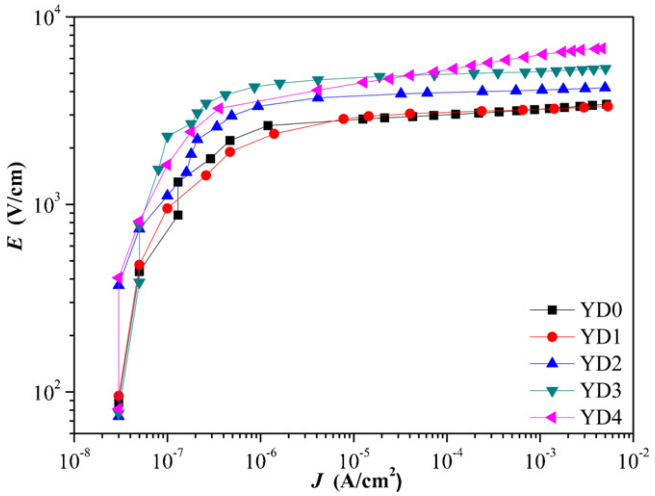

Fig. 4. Electric field–current density (E–J) characteristics of ZnO–Bi_2O_3-based varistor ceramics doped with various amounts of $Y(NO_3)_3{\cdot}6H_2O$.

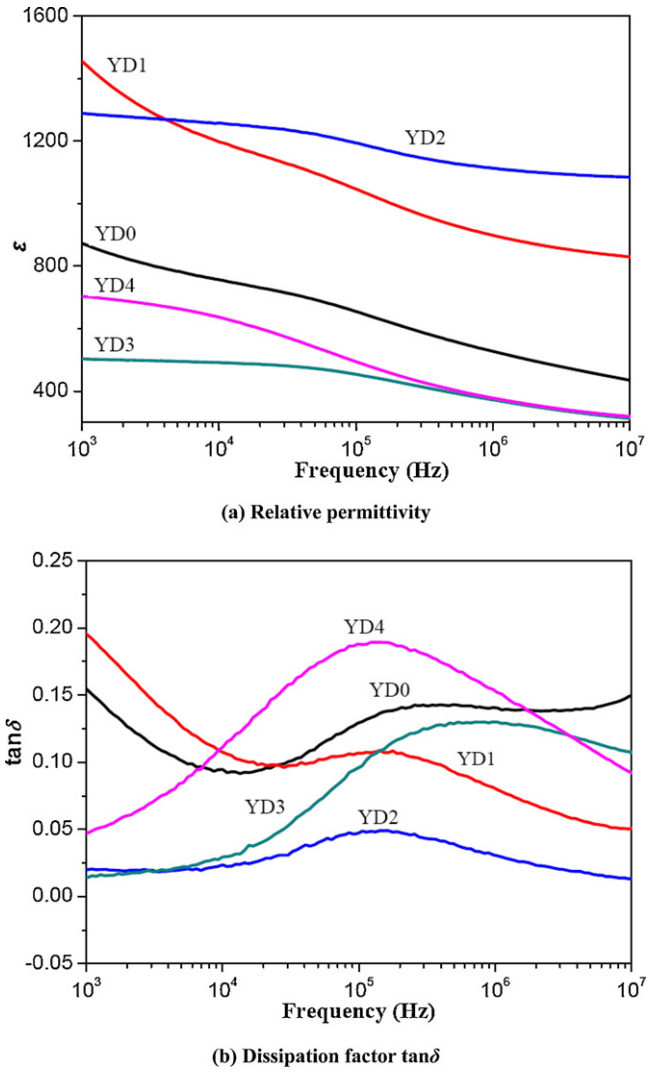

Fig. 5. Dielectric characteristics versus frequency of $Y(NO_3)_3{\cdot}6H_2O$ doped ZnO–Bi_2O_3-based varistor ceramics.

In all the samples, when the amount of YN dopant increases from 0 mol% to 2.0 mol%, I_L initially decreases and then increases. When the amount of YN is less than 0.40 mol%, I_L shows little change, but when the amount of YN is more than 0.40 mol%, I_L increases sharply by up to 1613% compared with I_L of the sample without YN. At the same time, when ZnO–Bi_2O_3-based varistor ceramics are doped with 2.00 mol% YN, there is an increase in the second phases, such as the $Zn_7Sb_2O_{12}$-type spinel phase and $Bi_3Zn_2Sb_3O_{14}$-type pyrochlore phase. With an increase in YN concentration, the amount of second phases increases and the microstructures become nonuniform. Consequently, α decreases, and I_L increases. In general, variation in I_L is opposite that of α. I_L is a result of most electrons passing over the Schottky barrier at grain boundaries. Therefore, the lower the barrier height, the higher I_L is, and the lower α is [12,29,35,39,40]. Decrease in I_L is attributed to an increase in activation energy (the average energy needed for electrons to overcome the Schottky barrier) and the homogeneous distribution of the limited amount of varistor dopants available in these samples. Inasmuch as I_L is directly related to degradation, which is discussed later on, I_L should be as low as possible for various applications [35].

Values of D_V first decrease and then increase with the addition of YN, and achieve a minimum value when the sample is doped with 0.16 mol% YN. The undoped sample is burst by short duration shocks of 1 kA, 8/20 μs, but samples doped with YN are not. Between 0.04 mol% and 0.16 mol% of YN, D_V is better (around 2%). However, beyond 0.16 mol%, it becomes higher (up to 74%). Therefore, degradation performance can be optimized by adding an appropriate concentration of YN.

Fig. 4 shows electric field–current density (E–J) curves of ZnO–Bi_2O_3-based varistor ceramics with various concentrations of YN. The curves show that conduction characteristics are divided into two regions, namely, a linear region before the breakdown field and a non-linear region after the breakdown field. The sharper the knee of the curves between the two regions, the better the non-linear property is [41]. In Fig. 4, E–J curves show that nonlinear properties increase in the order of YD2 → YD1 → YD3 → YD0 → YD4. V_T increases in the order of YD4 → YD3 → YD2 → YD0 → YD1, as shown in Table 1.

In addition, results also show that with the addition of 0.16 mol% YN, YN-doped ZnO–Bi_2O_3-based varistor ceramics exhibit comparatively better comprehensive electrical properties, and that the E–J curve is the best, with V_T at 425 V/mm, α at 73.9, I_L at 2.62 μA, and D_V at 1.7.

Fig. 5 shows the frequency dependence of the dielectric parameters of ZnO–Bi_2O_3-based varistor ceramics with various concentrations of YN. In the range of 1 kHz to 10 MHz, the doping of YN has a strong influence on an apparent dielectric constant, which decreases gradually as frequency increases. The property is associated with the polarization of dielectrics. In general, the apparent dielectric constant of ZnO–Bi_2O_3-based varistor ceramics is in the range of 1200–1400. Inasmuch as, of all the samples, only sample YD2, doped with 0.16 mol% YN, has an apparent dielectric constant in the range of 1200–1400, this sample has the best nonlinear performance. Variations in the dissipation factor, with an increase in frequency, form a complicated curve known as the dielectric dispersion phenomenon. Generally speaking, the dissipation factor decreases as frequency increases until a minimum is obtained, then it increases to a maximum before decreasing again. Abnormal dielectric dispersion is not seen clearly through an apparent dielectric constant curve, but is seen clearly at about 100 kHz from the dissipation factor. In general, peak of the dissipation factor is relatively low when a sharper dielectric dispersion, called abnormal dispersion, is not exhibited saliently in the range of 10^5–10^6 Hz [42–45].

4. Conclusions

The microstructure and electrical properties of ZnO–Bi_2O_3-based varistor ceramics doped with different concentrations of YN were investigated. With an increase of YN concentration, the relative density changed slightly from 93.5% to 94.9%, the threshold voltage was significantly increased from 340 to 679 V/mm, the nonlinear coefficient values first increased and then decreased in the range 12.7–73.9, while the leakage current first decreased then increased. With increasing amounts of YN in the starting composition, Y-containing Bi-rich, Y_2O_3, and Sb_2O_4 phases were formed, and the average grain size decreased. The results also showed that with the addition of 0.16 mol% YN, YN-doped ZnO-based varistor ceramics exhibit comparatively better comprehensive electrical properties, namely the threshold voltage was 425 V/mm, the nonlinear coefficient was 73.9, the leakage current was 1.78 μA and the degradation coefficient of 1.7. The dielectric characteristics and lightning surge test also received the same additional content of YN. The results confirmed that doping with rare earth nitrates instead of rare earth oxides is very promising route in preparing high-performance ZnO–Bi_2O_3-based varistor ceramics.

Acknowledgments

This work was financially supported by National Nature Science Foundation of China (50902061), State Key Laboratory of New Ceramic and Fine Processing Tsinghua University, State Key Laboratory of Electrical Insulation and Power Equipment (EIPE11204), Leading Academic Discipline Project of Shanghai Municipal Education Commission (J50102), State Key Laboratory of Inorganic Synthesis and Preparative Chemistry of Jilin University (2011-22), Universities Natural Science Research Project of Jiangsu Province (10KJD430002), Research Foundation of Jiangsu University (11JDG084), Industrial Center of Jiangsu University Undergraduate Practice-Innovation Training Project and Jiangsu University Undergraduate Practice-Innovation Training Project.

References

[1] H. Feng, Z. Peng, X. Fu, Z. Fu, C. Wang, L. Qi, H. Miao, J. Alloys Compd. 509 (2011) 7175–7180.
[2] Z.H. Wu, J.H. Fang, D. Xu, Q.D. Zhong, L.Y. Shi, Int. J. Miner. Metall. Mater. 17 (2010) 86–91.
[3] A.U. Ubale, V.P. Deshpande, J. Alloys Compd. 500 (2010) 138–143.
[4] C.W. Nahm, J. Alloys Compd. 490 (2010) L52–L54.
[5] K. Yuan, G. Li, L. Zheng, L. Cheng, L. Meng, Z. Yao, Q. Yin, J. Alloys Compd. 503 (2010) 507–513.
[6] Z. Peng, X. Fu, Y. Zang, Z. Fu, C. Wang, L. Qi, H. Miao, J. Alloys Compd. 508 (2010) 494–499.
[7] C.W. Nahm, J. Alloys Compd. 505 (2010) 657–660.
[8] H. Bastami, E. Taheri-Nassaj, J. Alloys Compd. 495 (2010) 121–125.
[9] F. Liu, G. Xu, L. Duan, Y. Li, Y. Li, P. Cui, J. Alloys Compd. 509 (2011) L56–L58.
[10] E. Savary, S. Marinel, F. Gascoin, Y. Kinemuchi, J. Pansiot, R. Retoux, J. Alloys Compd. 509 (2011) 6163–6169.
[11] S.C. Pillai, J.M. Kelly, D.E. McCormack, P. O'Brien, R. Ramesh, J. Mater. Chem. 13 (2003) 2586–2590.
[12] D. Xu, L.Y. Shi, Z.H. Wu, Q.D. Zhong, X.X. Wu, J. Eur. Ceram. Soc. 29 (2009) 1789–1794.
[13] D. Xu, X.N. Cheng, X.H. Yan, H.X. Xu, L.Y. Shi, Trans. Nonferr. Met. Soc. China 19 (2009) 1526–1532.
[14] G.D. Tang, S.P. Liu, X. Zhao, Y.G. Zhang, D.H. Ji, Y.F. Li, W.H. Qi, W. Chen, D.L. Hou, Appl. Phys. Lett. 95 (2009).
[15] S. Bernik, S. Macek, B. Ai, J. Eur. Ceram. Soc. 21 (2001) 1875–1878.
[16] S. Bernik, S. Macek, A. Bui, J. Eur. Ceram. Soc. 24 (2004) 1195–1198.
[17] C.W. Nahm, B.C. Shin, Mater. Lett. 57 (2003) 1322–1326.
[18] C.W. Nahm, Solid State Commun. 132 (2004) 213–218.
[19] C.W. Nahm, B.C. Shin, Ceram. Int. 30 (2004) 9–15.
[20] J.S. Park, Y.H. Han, K.H. Choi, J. Mater. Sci.-Mater. Electron. 16 (2005) 215–219.
[21] H.Y. Liu, X.M. Ma, D.M. Jiang, W.Z. Shi, J. Univ. Sci. Technol. B 14 (2007) 266–270.
[22] M. Houabes, R. Metz, Ceram. Int. 33 (2007) 1191–1197.
[23] J. Liu, J. Hu, J.L. He, Y.H. Lin, W.C. Long, Sci. China Ser. E 52 (2009) 3668–3673.
[24] J.L. He, J. Hu, Y.H. Lin, Sci. China Ser. E 51 (2008) 693–701.
[25] V. Gunay, O. Gelecek-Sulan, O.T. Ozkan, Ceram. Int. 30 (2004) 105–110.
[26] W. Onreabroy, N. Sirikulrat, A.P. Brown, C. Hammond, S.J. Milne, Solid State Ionics 177 (2006) 411–420.
[27] D. Xu, X.N. Cheng, M.S. Wang, L.Y. Shi, Adv. Mater. Res. 79–82 (2009) 2007–2010.
[28] S. Bernik, N. Daneu, J. Eur. Ceram. Soc. 27 (2007) 3161–3170.
[29] C. Leach, Z. Ling, R. Freer, J. Eur. Ceram. Soc. 20 (2000) 2759–2765.
[30] M. Peiteado, J.F. Fernandez, A.C. Caballero, J. Eur. Ceram. Soc. 27 (2007) 3867–3872.
[31] D. Xu, X.F. Shi, X.N. Cheng, J. Yang, Y.E. Fan, H.M. Yuan, L.Y. Shi, Trans. Nonferr. Met. Soc. China 20 (2010) 2303–2308.
[32] D. Xu, C. Zhang, X.N. Cheng, Y.E. Fan, T. Yang, H.M. Yuan, Adv. Mater. Res. 197–198 (2011) 302–305.
[33] M. Peiteado, M.A. de la Rubia, M.J. Velasco, F.J. Valle, A.C. Caballero, J. Eur. Ceram. Soc. 25 (2005) 1675–1680.
[34] M.A. de la Rubia, M. Peiteado, J.F. Fernandez, A.C. Caballero, J. Eur. Ceram. Soc. 24 (2004) 1209–1212.
[35] C.W. Nahm, C.H. Park, J. Mater. Sci. 35 (2000) 3037–3042.
[36] D. Xu, L.Y. Shi, X.X. Wu, Q.D. Zhong, High Volt. Eng. 35 (2009) 2366–2370.
[37] D.R. Clarke, J. Am. Ceram. Soc. 82 (1999) 485–502.
[38] P.R. Bueno, J.A. Varela, E. Longo, J. Eur. Ceram. Soc. 28 (2008) 505–529.
[39] C.W. Nahm, Solid State Commun. 149 (2009) 795–798.
[40] S. Bernik, G. Brankovic, S. Rustja, M. Zunic, M. Podlogar, Z. Brankovic, Ceram. Int. 34 (2008) 1495–1502.
[41] C.W. Nahm, Mater. Lett. 60 (2006) 3311–3314.
[42] C.W. Nahm, Mater. Chem. Phys. 82 (2003) 726–732.
[43] C.W. Nahm, Mat. Sci. Eng. B: Solid 133 (2006) 91–97.
[44] C.W. Nahm, Mater. Chem. Phys. 94 (2005) 275–282.
[45] C.M. Wang, J.F. Wang, H.C. Chen, W.B. Su, G.Z. Zang, P. Qi, B.Q. Ming, Solid State Commun. 132 (2004) 163–167.